NeuroImage 185 (2019) 191–197

Contents lists available at ScienceDirect

NeuroImage

journal homepage: www.elsevier.com/locate/neuroimage

Neural dynamics of verbal working memory processing in children and adolescents

Christine M. Embury [a,b,c], Alex I. Wiesman [a,b], Amy L. Proskovec [a,b,c], Mackenzie S. Mills [a,b], Elizabeth Heinrichs-Graham [a,b], Yu-Ping Wang [d], Vince D. Calhoun [e,f], Julia M. Stephen [e], Tony W. Wilson [a,b,*]

[a] Department of Neurological Sciences, University of Nebraska Medical Center, Omaha, NE, USA
[b] Center for Magnetoencephalography, University of Nebraska Medical Center, Omaha, NE, USA
[c] Department of Psychology, University of Nebraska Omaha, Omaha, NE, USA
[d] Department of Biomedical Engineering, Tulane University, New Orleans, LA, USA
[e] The Mind Research Network, Albuquerque, NM, USA
[f] Department of Electrical and Computer Engineering, University of New Mexico, Albuquerque, NM, USA

ARTICLE INFO

Keywords:
Working memory
MEG
Neuroimaging
Alpha
Oscillations
Dev-CoG

ABSTRACT

Development of cognitive functions and the underlying neurophysiology is evident throughout childhood and adolescence, with higher order processes such as working memory (WM) being some of the last cognitive faculties to fully mature. Previous functional neuroimaging studies of the neurodevelopment of WM have largely focused on overall regional activity levels rather than the temporal dynamics of neural component recruitment. In this study, we used magnetoencephalography (MEG) to examine the neural dynamics of WM in a large cohort of children and adolescents who were performing a high-load, modified verbal Sternberg WM task. Consistent with previous studies in adults, our findings indicated left-lateralized activity throughout the task period, beginning in the occipital cortices and spreading anterior to include temporal and prefrontal cortices during later encoding and into maintenance. During maintenance, the occipital alpha increase that has been widely reported in adults was found to be relatively weak in this developmental sample, suggesting continuing development of this component of neural processing, which was supported by correlational analyses. Intriguingly, we also found sex-specific developmental effects in alpha responses in the right inferior frontal region during encoding and in parietal and occipital cortices during maintenance. These findings suggested a developmental divergence between males and females in the maturation of neural circuitry serving WM during the transition from childhood to adolescence.

1. Introduction

Working memory involves the real-time processing and retention of incoming stimuli, using temporary storage and manipulation mechanisms to reactivate and maintain neural representations. Working memory (WM) processing is typically dissected into three phases: encoding, maintenance and retrieval. Encoding broadly applies to the process of loading relevant stimuli into a temporary buffer, while maintenance corresponds to the short-term retention and manipulation of the loaded representations, and finally, retrieval is the process of utilizing these representations to recall or recognize the stimuli to achieve current task goals (Baddeley, 1992). Many studies examining the underlying neurophysiology of WM in healthy adults have found widespread activity in frontal-parietal networks, superior temporal and occipital cortices, and the cerebellum, with clear lateralization on domain-specific tasks (e.g., verbal versus visuospatial; Cabeza and Nyberg, 2000; Heinrichs-Graham and Wilson, 2015; Rottschy et al., 2012). In addition, studies of the neural oscillatory dynamics serving WM processing have implicated broad alpha frequency (8–16 Hz) activity in these neural regions as being essential for task performance (Bonnefond and Jensen, 2012; Handel et al., 2011; Heinrichs-Graham and Wilson, 2015; Jensen et al., 2002; Jensen and Mazaheri, 2010; Proskovec et al., 2016; Roux and Uhlhaas, 2014).

Previous studies of WM in children and adolescents have found

* Corresponding author. Center for Magnetoencephalography, University of Nebraska Medical Center, 988422 Nebraska Medical Center, Omaha, NE, 68198, USA.
E-mail address: twwilson@unmc.edu (T.W. Wilson).

https://doi.org/10.1016/j.neuroimage.2018.10.038
Received 9 March 2018; Received in revised form 9 October 2018; Accepted 13 October 2018
Available online 16 October 2018

mostly similar, albeit more widespread patterns of brain activity relative to adults, with this more extensive recruitment thought to reflect inefficiencies in developing brain networks (Bathelt et al., 2018; Jolles et al., 2011). Most developmental studies of WM and other higher order cognitive functions have found that these processes continue to develop into late adolescence (Andre et al., 2016; Brahmbhatt et al., 2008; Peters et al., 2014; Thomason et al., 2009; Vogan et al., 2016), however many of these studies focused on the visuospatial component of WM processing (Andre et al., 2016; Conklin et al., 2007; Darki and Klingberg, 2015; Klingberg, 2006; Olesen et al., 2007; Scherf et al., 2006). Studies of verbal WM in particular have been far less numerous, but several functional MRI (fMRI) studies have evaluated WM processing in children, and broadly these studies have shown developmental alterations between children and adults in the frontal, parietal, and cerebellar regions responding to memory load manipulations (O'Hare et al., 2008; Thomason et al., 2009; Vogan et al., 2016).

Developmental sex differences have previously been found in behavioral studies of attention, psychomotor, and memory measures (Gur et al., 2012; Gur and Gur, 2016; Malagoli and Usai, 2018). Some of these differences in performance have been linked to structural and resting-state functional brain differences between male and female youth (Gur and Gur, 2016). Basically, fMRI and behavioral studies of adolescence have found sex differences in a variety of higher order cognitive functions, including WM (Gur and Gur, 2016; Zilles et al., 2016), but the oscillatory dynamics underlying these differences have not been examined and remain poorly understood.

In the current study, we examined the neurophysiology of verbal WM using high-density magnetoencephalography (MEG) in a large cohort of children and young adolescents aged 9–14 years. Participants completed a high-load, modified Sternberg verbal WM task during MEG, and we identified the specific neural oscillatory responses corresponding to verbal WM encoding and maintenance processes. In addition, our large sample size allowed for the investigation of sex differences in the development of WM processing. We hypothesized that, consistent with previous adult findings in similar tasks, adolescents would show a characteristic left-lateralized response, but would also recruit additional areas, including right homologue regions, to complete task goals. We further hypothesized that as age increased, specific neural component recruitment would decrease in strength with increasing development, consistent with the consolidation of the underlying networks, and that the pattern of regional recruitment would differ by sex as age increased, showing a divergent pattern of neural maturation in adolescence.

2. Methods

2.1. Participants

Ninety-five participants completed the verbal WM task as part of the National Science Foundation (NSF)-funded Developmental Chronnecto-Genomics (Dev-CoG) study. All participants were recruited from the University of Nebraska Medical Center (UNMC) site and were between the ages of 9 and 14 years ($M_{age} = 11.22$, $SD_{age} = 1.54$; 47 females). Participants were typically developing, without attention-deficit/hyperactivity disorder (ADHD) or other disorders affecting brain function, mental illness or previous head trauma, and identified English as their primary language. Participants were excluded according to general MEG/MRI exclusionary criteria such as the presence of metal implants, dental braces or permanent retainers, or other metallic or otherwise magnetic non-removable devices. Other exclusionary criteria included major medical conditions such as cancer, history or diagnosis of alcohol or substance use disorder, or pregnancy. All procedures were approved by the UNMC Institutional Review Board and informed consent from the child's parent or legal guardian, as well as assent from the child, was obtained before proceeding with the study.

2.2. Procedure

2.2.1. Task paradigm

Participants were shown a centrally-presented fixation cross embedded in a 3 × 2 grid for 1.3 s (Fig. 1). An array of six consonants then appeared at fixed locations within the grid for 2.0 s (i.e., encoding). Following, the letters disappeared and the empty grid remained on the screen for 3.0 s (i.e., maintenance). A single probe letter then appeared in the grid for 0.9 s, and the participant was instructed to respond by button press with their right index or middle finger as to whether the probe was in or out of the previous array of letters. A total of 128 trials were completed, equally split and pseudorandomized between in- and out-of-set trials, for a total run time of about 15 min. Responses were recorded concomitantly with the MEG data, with accuracy and reaction time to be determined offline. This task has been utilized in several previous studies of adults (Heinrichs-Graham and Wilson, 2015; Proskovec et al., 2016; Wiesman et al., 2016; Wilson et al., 2017). Using signal detection theory, participants' responses were categorized into hits (correctly responding in-set to an in-set probe stimulus), misses (incorrectly responding out-of-set to an in-set probe stimulus), false alarms (incorrectly responding in-set to an out-of-set probe stimulus), and correct rejections (correctly responding out-of-set to an out-of-set probe stimulus). To calculate each participant's d' value, or the likelihood of correctly identifying an in-set probe stimulus, we subtracted the normalized false alarm rate from the normalized hit rate. Participants were excluded from analyses for d' values of less than 1 SD below the full group mean.

2.2.2. MEG data acquisition

MEG recordings were conducted in a one-layer magnetically shielded room with active shielding engaged. Neuromagnetic responses were acquired with an Elekta MEG system with 306 magnetic sensors (204 planar gradiometers, 102 magnetometers; Elekta, Helsinki, Finland) using a bandwidth of 0.1–330 Hz, sampled continuously at 1 kHz. Each participant's data were individually corrected for head motion, and noise reduction was applied using the signal space separation method with a temporal extension (tSSS; Taulu and Simola, 2006; Taulu et al., 2005).

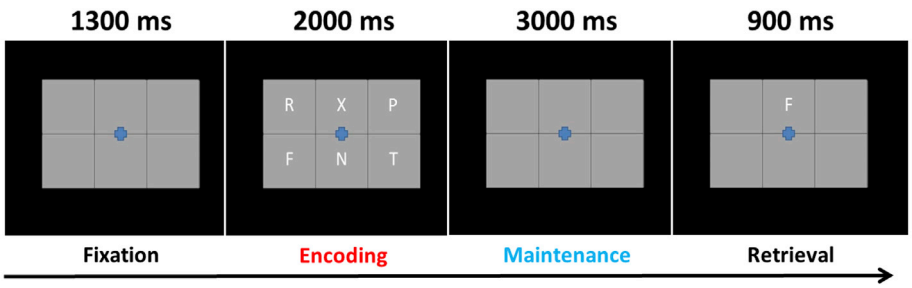

Fig. 1. Working memory task paradigm. Presentation started with a fixation cross shown over an empty 3 × 2 grid, followed by the appearance of six consonants within the grid for 2 s (encoding), an empty grid for 3 s (maintenance), and finally a probe letter in the grid (retrieval). During the retrieval phase, participants were to respond by button press as to whether the probe letter was present or absent in the original encoding set of six consonants.

2.2.3. MEG coregistration and structural MRI processing

Preceding MEG measurement, four coils were attached to the participant's head and localized, together with the three fiducial points and scalp surface, using a 3-D digitizer (Fastrak 3SF0002, Polhemus Navigator Sciences, Colchester, VT, USA). Once the participant was positioned for MEG recording, an electric current with a unique frequency label (e.g., 322 Hz) was fed to each of the coils. This induced a measurable magnetic field and allowed each coil to be localized in reference to the sensors throughout the recording session. Since coil locations were also known in head coordinates, all MEG measurements could be transformed into a common coordinate system. With this coordinate system, each participant's MEG data were coregistered with their individual structural T1-weighted MRI data prior to source space analyses using BESA MRI (Version 2.0). Structural T1-weighted MRI images were acquired using a Siemens Skyra 3-T MRI scanner with a 32-channel head coil and a MP-RAGE sequence with the following parameters: TR = 2400 ms; TE = 1.94 ms; flip angle = 8°; FOV = 256 mm; slice thickness = 1 mm (no gap); voxel size = 1 × 1 × 1 mm. These data were aligned in parallel to the anterior and posterior commissures and transformed into standardized space. Following source analysis (i.e., beamforming), each participant's 4.0 × 4.0 × 4.0 mm functional images were also transformed into standardized space using the transform that was previously applied to the structural MRI volume and spatially resampled.

2.2.4. MEG time-frequency transformation and statistics

Cardiac artifacts were removed from the data using signal-space projection (SSP), which was accounted for during source reconstruction (Uusitalo and Ilmoniemi, 1997). The continuous magnetic time series was divided into epochs of 7.2 s duration, with the baseline being defined as −0.4 to 0.0 s before the onset of the encoding grid. Epochs containing artifacts (e.g., eye blinks, muscle artifacts, eye saccades, swallowing, coughing) were rejected based on a fixed-threshold method, supplemented with visual inspection. Briefly, the distribution of amplitude and gradient values per participant was computed using all trials, and the highest amplitude/gradient trials relative to the total distribution were excluded by selecting a threshold that rejected extreme values. Notably, thresholds are set for each participant due to differences among individuals in head size and sensor proximity, which strongly affect MEG signal amplitude. Trials were also randomly excluded from participants with the highest total trial counts so that the total number of accepted trials used in the final analyses did not differ by age. An average of 95.2 ($SD = 9.7$) trials were used for further analysis, and a one-way ANOVA of number of trials included by age in years revealed that this did not statistically differ by age ($F = 1.15$; $p = .346$).

Artifact-free epochs were transformed into the time-frequency domain using complex demodulation (resolution: 1.0 Hz, 50 ms; Papp and Ktonas, 1977), and the resulting spectral power estimations per sensor were averaged over trials to generate time-frequency plots of mean spectral density. These sensor-level data were normalized using the respective bin's baseline power, which was calculated as the mean power during the −0.4 to 0 s time period. The specific time-frequency windows used for imaging were determined by statistical analysis of the sensor-level spectrograms across the entire array of gradiometers during the 5.0 s "encoding" and "maintenance" time windows (Fig. 1). To reduce the risk of false-positive results while maintaining reasonable sensitivity, a two-stage procedure was followed to control for Type 1 error. In the first stage, two-tailed one-sample *t*-tests were conducted on each data point and the output spectrograms of t-values were thresholded at $p < .05$ to define time-frequency bins containing potentially significant oscillatory deviations across all participants. In stage two, the time-frequency bins that survived the threshold were clustered with temporally and/or spectrally neighboring bins that were also above the ($p < .05$) threshold, and a cluster value was derived by summing all the *t*-values of all data points in the cluster. Nonparametric permutation testing was then used to derive a distribution of cluster values and the significance level of the observed clusters (from stage one) was tested directly using this distribution (Ernst, 2004; Maris and Oostenveld, 2007). For each comparison, at least 10,000 permutations were computed to build a distribution of cluster values. Based on these analyses, the time-frequency windows that contained significant oscillatory events across all participants during the encoding and maintenance phases were subjected to the beamforming analysis (see Results, Section 3.2).

2.2.5. MEG source imaging and statistics

Cortical activity were imaged through an extension of the linearly constrained minimum variance vector beamformer (Gross et al., 2001; Hillebrand et al., 2005; Van Veen et al., 1997), which employs spatial filters in the frequency domain to calculate source power for the entire brain volume. The single images are derived from the cross-spectral densities of all combinations of MEG gradiometers averaged over the time-frequency range of interest, and the solution of the forward problem for each location on a grid specified by input voxel space. This use of the cross-spectral densities is often referred to as the dynamic imaging of coherent sources (DICS) beamformer (Gross et al., 2001). Following convention, we computed noise-normalized, source power per voxel in each participant using active (i.e., task) and passive (i.e., baseline) periods of equal duration and bandwidth (Hillebrand et al., 2005). Such images are typically referred to as pseudo-*t* maps, with units (i.e., pseudo-*t*) that reflect noise-normalized power differences (i.e., active vs. passive) per voxel. MEG preprocessing and imaging used the BESA (V 6.1) software.

Normalized differential source power was computed for the statistically-selected time-frequency bands (see below), using a common baseline, over the entire brain volume per participant at 4.0 × 4.0 × 4.0 mm resolution. The resulting 3D maps of brain activity were averaged across participants to assess the neuroanatomical basis of significant oscillatory responses identified through the sensor-level analysis. Next, whole brain correlations were generated between the participant-level maps and age in months to examine developmental changes in the neural responses of males and females separately. To statistically compare these sex specific correlations, we computed voxel-wise Fisher *Z* tests (thresholded at $p < .001$) between the whole-brain correlation maps for each sex, which represent age-by-sex interactions in the oscillatory coding of verbal WM. Maps were corrected for multiple comparisons using a cluster correction threshold of 300 contiguous voxels, which was a conservative estimate based on the spatial smoothness of the image.

3. Results

3.1. Demographic data and behavioral results

Of the 95 participants who completed the task, 16 participants were excluded for d' values less than one standard deviation below the mean ($M_{d'} = 1.22$, $SD_{d'} = 0.695$), and an additional 21 participants were excluded during MEG preprocessing and analysis due to excessive motion and/or other MEG artifacts. A cohort of 58 participants were used in the final analyses ($M_{age} = 11.78$ years, $SD_{age} = 1.59$; 30 females, 28 males). Importantly, the age distribution of these participants did not differ between sexes, $t = -1.23$, $p = .224$.Average accuracy rate for the 58 participants was 70.83 ± 10.59%, with a correct mean hit rate of 0.72, a mean false alarm rate of 0.21, an average reaction time of 1061.78 ± 229.43 ms, and an average $d' = 1.48$. All artifact-free trials were utilized in the final MEG analyses to maximize the signal to noise ratio (SNR), although we conducted preliminary analyses both ways (with and without incorrect trials) and the results were very similar. As stated in the methods, the number of trials included in the final analyses did not significantly differ by age.

There was a significant correlation between age in months and accuracy, such that as age increased, accuracy rates also increased, $r = 0.42$, $p < .001$ (see Fig. 2). Further, the correlation between age in months and reaction time was significant, such that as age increased, reaction time decreased, $r = -0.40$, $p = .002$ (see Fig. 2). Accuracy and reaction time

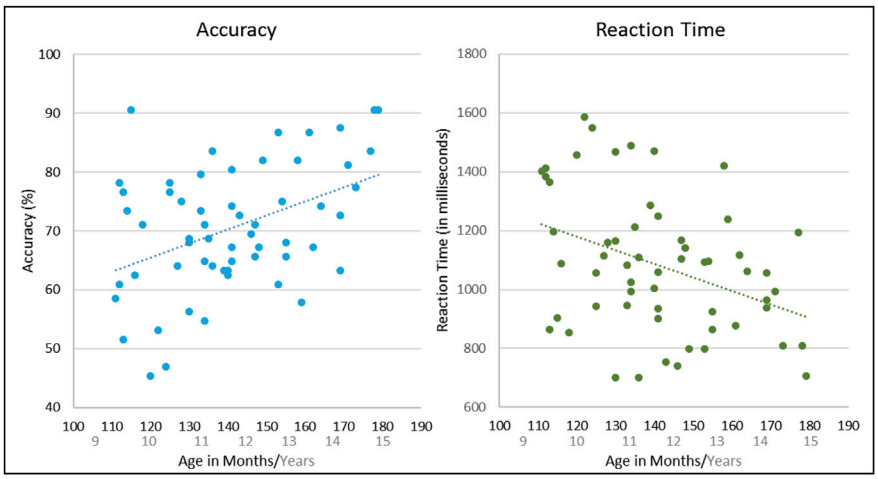

Fig. 2. Behavioral correlations. *Left*: Age in months and accuracy were significantly correlated, such that as age increased, accuracy increased, $r = 0.42$, $p < .001$. *Right*: Age in months also significantly correlated with reaction time, such that as age increased, reaction time decreased, $r = -0.40$, $p = .002$. These behavioral data show a clear developmental curve, where performance improves with age.

were also significantly correlated, such that as accuracy increased, reaction time decreased, $r = -0.59$, $p < .001$ (i.e., the opposite of a speed-accuracy tradeoff; see Supplementary Fig. S1). Notably, there was no significant age by sex interaction in any of the behavioral metrics examined (accuracy: $F = 1.67$, $p = .111$; reaction time: $F = 1.37$, $p = .218$; d': $F = 1.67$, $p = .111$).

3.2. Sensor-level results

Statistical evaluation of the time-frequency spectrograms showed a significant alpha decrease throughout the encoding period from 9 to 16 Hz in posterior and left hemispheric sensors, and a significant alpha increase from 8 to 11 Hz during maintenance in posterior sensors ($p < .001$, corrected; Fig. 3). Time-frequency bins were broken into 400 ms windows of 9–16 Hz from 200 to 2200 ms and 8–11 Hz from 3400 to 5000 ms. Each 400 ms window was reconstructed in source space using a beamformer to identify the neural regions underlying these responses.

3.3. Source-level results

Average beamformer images across all participants revealed a broad alpha decrease in left hemispheric brain regions throughout most of the task. This alpha decrease initially emerged in the bilateral occipital cortices, and then extended anteriorly with time to include left temporal and inferior frontal regions, with activity concentrated in these latter regions throughout mid to late maintenance periods, as shown in Fig. 4.

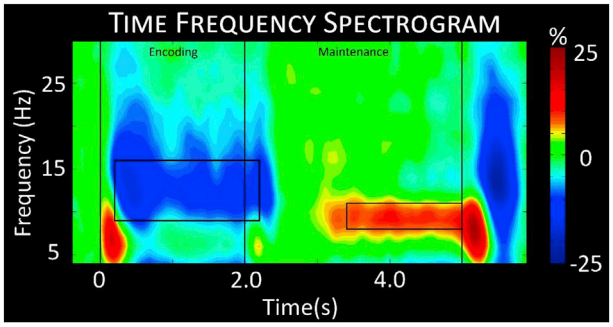

Fig. 3. Time-frequency spectrogram. A grand-averaged time-frequency spectrogram from a representative sensor (M2313) near the parieto-occipital cortices. The same sensor was chosen in each participant. Time is shown on the x-axis in seconds, while frequency is shown on the y-axis in Hz. The colors reflect power increases (red) and decreases (blue) relative to the baseline, with the scale bar shown to the far right. A significant decrease in alpha from 9 to 16 Hz can be discerned throughout encoding into early maintenance, followed by a significant alpha increase throughout mid to late maintenance in a more narrow 8–11 Hz range. Time-frequency windows for source imaging (beamforming) were derived from statistical analysis of the sensor-level spectrogram data, and these windows are demarcated by the black boxes.

In addition, there was an increase in alpha observed during the maintenance period, especially during later time bins, and this was primarily generated by bilateral parieto-occipital cortices (see Fig. 5). Next, we

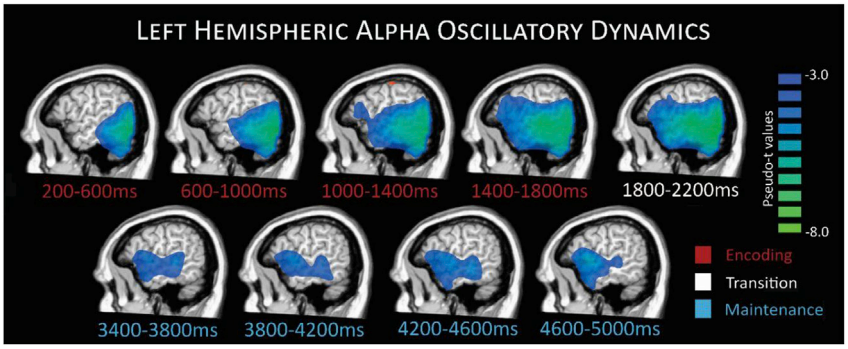

Fig. 4. Left hemispheric alpha oscillatory dynamics. Group averaged images per time window during encoding (time bin shown in red), transition (white), and maintenance (blue) periods depict the progression of responses during task performance. A strong decrease in alpha activity relative to the baseline can be seen during encoding time bins starting in occipital and stretching forward to more temporal and prefrontal regions through later encoding, transition, and into maintenance.

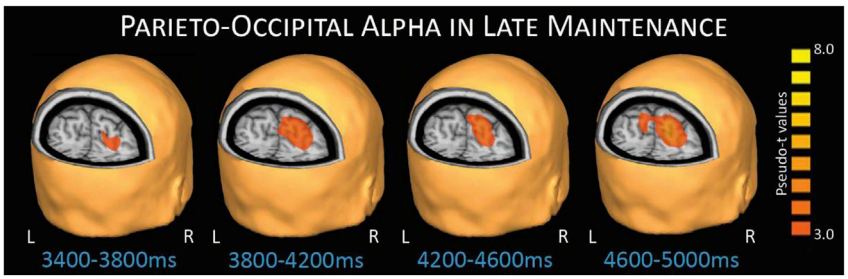

Fig. 5. Parieto-occipital alpha during late maintenance. This response extended through most of the maintenance phase and has been reported in previous working memory studies focused on adults. The response is believed to be related to the ability to suppress incoming visual information, thereby maintaining the integrity of the target stimuli representations.

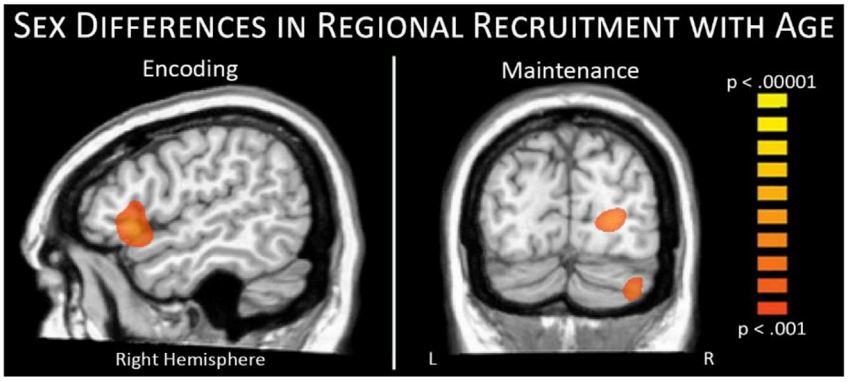

Fig. 6. Sex differences in regional recruitment with age. During encoding stronger alpha decreases with age were observed in the right inferior frontal region of females (left), while during maintenance stronger alpha increases with age were observed in parietal, occipital, and cerebellar regions of males (right).

investigated the impact of age and sex on these neuronal dynamics. First, we computed whole-brain correlation maps with age for each time-frequency bin imaged, controlling for reaction time. No significant correlations between age and neural oscillatory activity, accounting for reaction time, were found in the full sample (i.e., across both sexes). We further examined whether biological sex differentially influenced the effects of age on neural oscillatory activity. As mentioned above, age distribution did not differ by sex, $t = -1.23$, $p = .224$. Interestingly, we found significant sex-by-age interaction differences in multiple brain regions during encoding and maintenance (see Fig. 6 and Supplementary Fig. S2).

Specifically, during encoding, we detected a significant age-by-sex interaction within the right inferior frontal cortex, $Z = 3.85$, $p < .001$, where females showed a stronger negative correlation between age in months and neural activity, whereas males had a weaker positive relationship. It should be noted that, since the alpha response during this time period (i.e., encoding) was a decrease from baseline, this finding should be interpreted as females exhibiting a stronger response with increasing age, with the opposite effect found for males. Follow-up Pearson correlations suggested this stronger alpha response in females was associated with higher *d'* scores, $r = -.42$, $p < .05$, while males exhibited no relationship with performance.

During maintenance, three posterior peaks showed sex-specific developmental effects, including peaks in the right occipital cortex ($Z = 4.07$, $p < .001$), right cerebellum ($Z = 3.79$, $p < .001$), and parietal regions ($Z = 4.26$, $p < .001$). In these regions, males exhibited a stronger alpha increase with increasing age in months, while females showed a weaker negative relationship. Since the alpha response in these regions during the maintenance period was an increase from baseline, this finding should be interpreted as males exhibiting a stronger response with increasing age.

Follow-up Pearson correlations indicated alpha activity in these regions was not significantly correlated with behavioral performance in either group.

4. Discussion

In the current study, we used high-density MEG to characterize the neural dynamics of the encoding and maintenance phases of WM during the transition from childhood to adolescence. Behaviorally, we found that as age increased, accuracy increased and reaction time decreased, reflecting a strong developmental improvement across this age range. In regards to the neural mechanisms, our data showed a largely left lateralized response with an occipital alpha decrease early-on that extended into left temporal and prefrontal cortices during later encoding and maintenance, followed by a parieto-occipital alpha increase during middle and later maintenance. As predicted, this general pattern of activity was consistent with previous studies in adults (Cabeza and Nyberg, 2000; Heinrichs-Graham and Wilson, 2015; Proskovec et al., 2016; Rottschy et al., 2012; Wilson et al., 2016), as well as this age group (Bathelt et al., 2018; Brahmbhatt et al., 2008; Kharitonova et al., 2015; Nagel et al., 2013; Thomason et al., 2009; Vogan et al., 2016), although the temporal evolution of these dynamics have not been previously evaluated in a youth sample. In addition, we found that WM related oscillations were altered by development, but interestingly these developmental effects were all sex-specific suggesting a divergence in this age range between males and females. Below, we discuss the implications of these findings for understanding changes in WM performance and oscillatory activity during the emergence of sex differences during adolescence.

Critically, all of the developmental effects observed in this study were sex-specific, which was not altogether surprising given the age range of our participants and known sex differences in behavior and physiology during adolescence. In particular, we found stronger recruitment of right inferior prefrontal regions in females during the encoding phase, and stronger alpha increases in posterior regions of males during maintenance. Previous studies have shown that more widespread prefrontal recruitment reflects inefficiencies in systems that are still under development (Bathelt et al., 2018; Jolles et al., 2011), although given the

overall age-related improvements in performance and our follow-up correlational analyses we propose that this increased recruitment in females had a positive effect, analogous to the greater recruitment of right hemispheric prefrontal areas seen in healthy aging (Proskovec et al., 2016). Essentially, WM studies of healthy aging have shown that greater involvement of right hemispheric homologue regions is generally associated with preserved performance in older adults (Cabeza et al., 2002; Emery et al., 2008; Proskovec et al., 2016; Reuter-Lorenz et al., 2000). In male participants, we found increased alpha activity during maintenance in posterior regions, including occipital, parietal, and cerebellar cortices. Such activity has previously been related to the ability to inhibit the processing of incoming visual stimuli, which is thought to be critical for maintaining the integrity of representations held in WM (Andre et al., 2016; Bonnefond and Jensen, 2012, 2013; Handel et al., 2011; Payne et al., 2013). Thus, increases in parietal and occipital alpha with age likely reflect improved suppression of incoming visual information during maintenance in males, which would enhance WM task performance. Surprisingly, females exhibited developmental effects in the opposite direction (i.e., reduced occipital alpha with increasing age). This could indicate that WM network maturational patterns during the adolescent transition differ in males and females, with prefrontal development leading in females and parieto-occipital circuits leading in males. Such sex differences in parieto-occipital circuits may explain why the alpha increases in these regions across all participants were qualitatively weaker than observed in previous studies of adults. The weakness of this response throughout maintenance was particularly noteworthy, as it is a prominent, robust response in verbal WM studies in adults (Heinrichs--Graham and Wilson, 2015; McDermott et al., 2016; Proskovec et al., 2016; Wiesman et al., 2016; Wilson et al., 2017). Future studies focusing on later adolescence and early adulthood should continue to focus on this response, and thereby map its full developmental trajectory. We would hypothesize that the response pattern in males and females would converge by early adulthood, as sex differences in the occipital alpha increase have not been previously reported in adults. Finally, cerebellar activity found during maintenance also differed by sex, and such right cerebellar activity is consistent with the literature (Brahmbhatt et al., 2008; Cabeza and Nyberg, 2000; Heinrichs-Graham and Wilson, 2015; McDermott et al., 2017; Ng et al., 2016).

The neural dynamics observed in these children and adolescents follows the adult literature and the established Baddeley model of WM (Baddeley, 1992, 2000), including the central executive, phonological loop, and visuospatial sketchpad components. Briefly, multiple studies have connected activity in superior temporal and inferior frontal cortices to verbal processing and subvocal rehearsal mechanisms, consistent with operation of the phonological loop component of WM processing (Heinrichs-Graham and Wilson, 2015; Proskovec et al., 2016; Rottschy et al., 2012; Wilson et al., 2017). Prefrontal and posterior cortical activity has previously been linked to executive level processing (prefrontal), and potentially top-down modulation of parieto-occipital alpha to suppress incoming visual information from disturbing representations currently held in the so-called slave systems (Andre et al., 2016; Bathelt et al., 2018; Bonnefond and Jensen, 2012, 2013; Handel et al., 2011; Jolles et al., 2011; Payne et al., 2013). In line with previous studies, we found this executive component of WM processing to be more dynamic within this age range, suggesting continuing development of these neural and cognitive faculties during the transition from childhood to adolescence.

One limitation of the current study is that our high-load verbal WM task was very difficult for participants, with the youngest participants exhibiting lower accuracy rates. To maintain a reasonable SNR for our MEG analyses and to avoid age-related differences in the number of accepted trials, we opted to include both correct and incorrect trials in our final analyses. This practice is common in the neuroimaging literature, but does raise concerns regarding the impact of accuracy on the neural responses. Importantly, in the current study, we ran the analysis both ways (i.e., correct trials only vs. correct + incorrect trials), and the results were very similar; thus, ultimately this aspect of the analysis had a negligible impact on the results. Additionally poor task performance led to a high number of exclusions at early stages of analysis, a limitation that should be addressed in future studies. Another possible limitation is that we did not perform any direct comparisons with adult WM responses. Such responses are well characterized in adults (Cabeza and Nyberg, 2000; Heinrichs--Graham and Wilson, 2015; Jensen et al., 2002; Proskovec et al., 2016; Rottschy et al., 2012), but future studies should include an adult group and/or longitudinal designs so that the overall trajectory is further clarified. Finally, the current study did not examine the direct involvement of sex hormones in this age range, and their role should be addressed in future studies of sex differences in cognitive and neural development.

In conclusion, defining the underlying oscillatory mechanisms of WM processing in terms of encoding and maintenance operations allows a more refined characterization of the development of this cognitive capacity. Our study used MEG to examine the neural dynamics of these responses, finding many similarities with previous studies in adults, as well as some minor divergence. Overall, the findings were broadly consistent with the existing literature, showing continual development of both the behavioral and neural components in this age range. Finally, our data showed sex-specific differences in the development of key oscillatory responses serving WM processing, which is a novel finding that holds major implications for understanding the developmental trajectory of WM performance, dynamics, and circuitry.

Acknowledgements

This work was supported by a grant from the National Science Foundation (#1539067), the National Institute of Mental Health (R01MH103220), the National Institute on Aging (F31- AG055332), the National Institute of General Medical Sciences (P20GM103472), the National Institute of Biomedical Imaging and Bioengineering (R01EB020407) and by a Research Support Fund grant from the Nebraska Health System. The funders had no role in study design, data collection and analysis, decision to publish, or preparation of the manuscript. All authors declare no conflicts of interest.

Appendix A. Supplementary data

Supplementary data to this article can be found online at https://doi.org/10.1016/j.neuroimage.2018.10.038.

References

Andre, J., Picchioni, M., Zhang, R., Toulopoulou, T., 2016. Working memory circuit as a function of increasing age in healthy adolescence: a systematic review and meta-analyses. Neuroimage Clin. 12, 940–948.
Baddeley, A., 1992. Working memory. Science 255, 556–559.
Baddeley, A., 2000. The episodic buffer: a new component of working memory? Trends Cognit. Sci. 4, 417–423.
Bathelt, J., Gathercole, S.E., Johnson, A., Astle, D.E., 2018. Differences in brain morphology and working memory capacity across childhood. Dev. Sci. 21, e12579.
Bonnefond, M., Jensen, O., 2012. Alpha oscillations serve to protect working memory maintenance against anticipated distracters. Curr. Biol. 22, 1969–1974.
Bonnefond, M., Jensen, O., 2013. The role of gamma and alpha oscillations for blocking out distraction. Commun. Integr. Biol. 6, e22702.
Brahmbhatt, S.B., McAuley, T., Barch, D.M., 2008. Functional developmental similarities and differences in the neural correlates of verbal and nonverbal working memory tasks. Neuropsychologia 46, 1020–1031.
Cabeza, R., Anderson, N.D., Locantore, J.K., McIntosh, A.R., 2002. Aging gracefully: compensatory brain activity in high-performing older adults. Neuroimage 17, 1394–1402.
Cabeza, R., Nyberg, L., 2000. Imaging cognition II: an empirical review of 275 PET and fMRI studies. J. Cognit. Neurosci. 12, 1–47.
Conklin, H.M., Luciana, M., Hooper, C.J., Yarger, R.S., 2007. Working memory performance in typically developing children and adolescents: behavioral evidence of protracted frontal lobe development. Dev. Neuropsychol. 31, 103–128.
Darki, F., Klingberg, T., 2015. The role of fronto-parietal and fronto-striatal networks in the development of working memory: a longitudinal study. Cerebr. Cortex 25, 1587–1595.
Emery, L., Heaven, T.J., Paxton, J.L., Braver, T.S., 2008. Age-related changes in neural activity during performance matched working memory manipulation. Neuroimage 42, 1577–1586.

Ernst, M.D., 2004. Permutation methods: a basis for exact inference. Stat. Sci. 19, 676–685.
Gross, J., Kujala, J., Hamalainen, M., Timmermann, L., Schnitzler, A., Salmelin, R., 2001. Dynamic imaging of coherent sources: studying neural interactions in the human brain. Proc. Natl. Acad. Sci. U. S. A. 98, 694–699.
Gur, R.C., Richard, J., Calkins, M.E., Chiavacci, R., Hansen, J.A., Bilker, W.B., Loughead, J., Connolly, J.J., Qiu, H., Mentch, F.D., Abou-Sleiman, P.M., Hakonarson, H., Gur, R.E., 2012. Age group and sex differences in performance on a computerized neurocognitive battery in children age 8-21. Neuropsychology 26, 251–265.
Gur, R.E., Gur, R.C., 2016. Sex differences in brain and behavior in adolescence: findings from the philadelphia neurodevelopmental cohort. Neurosci. Biobehav. Rev. 70, 159–170.
Handel, B.F., Haarmeier, T., Jensen, O., 2011. Alpha oscillations correlate with the successful inhibition of unattended stimuli. J. Cognit. Neurosci. 23, 2494–2502.
Heinrichs-Graham, E., Wilson, T.W., 2015. Spatiotemporal oscillatory dynamics during the encoding and maintenance phases of a visual working memory task. Cortex 69, 121–130.
Hillebrand, A., Singh, K.D., Holliday, I.E., Furlong, P.L., Barnes, G.R., 2005. A new approach to neuroimaging with magnetoencephalography. Hum. Brain Mapp. 25, 199–211.
Jensen, O., Gelfand, J., Kounios, J., Lisman, J.E., 2002. Oscillations in the alpha band (9-12 Hz) increase with memory load during retention in a short-term memory task. Cerebr. Cortex 12, 877–882.
Jensen, O., Mazaheri, A., 2010. Shaping functional architecture by oscillatory alpha activity: gating by inhibition. Front. Hum. Neurosci. 4, 186.
Jolles, D.D., Kleibeuker, S.W., Rombouts, S.A., Crone, E.A., 2011. Developmental differences in prefrontal activation during working memory maintenance and manipulation for different memory loads. Dev. Sci. 14, 713–724.
Kharitonova, M., Winter, W., Sheridan, M.A., 2015. As working memory grows: a developmental account of neural bases of working memory capacity in 5- to 8-year old children and adults. J. Cognit. Neurosci. 27, 1775–1788.
Klingberg, T., 2006. Development of a superior frontal-intraparietal network for visuo-spatial working memory. Neuropsychologia 44, 2171–2177.
Malagoli, C., Usai, M.C., 2018. The effects of gender and age on inhibition and working memory organization in 14- to 19-year-old adolescents and young adults. Cognit. Dev. 45, 10–23.
Maris, E., Oostenveld, R., 2007. Nonparametric statistical testing of EEG- and MEG-data. J. Neurosci. Meth. 164, 177–190.
McDermott, T.J., Badura-Brack, A.S., Becker, K.M., Ryan, T.J., Khanna, M.M., Heinrichs-Graham, E., Wilson, T.W., 2016. Male veterans with PTSD exhibit aberrant neural dynamics during working memory processing: an MEG study. J. Psychiatr. Neurosci. 41, 251–260.
McDermott, T.J., Wiesman, A.I., Proskovec, A.L., Heinrichs-Graham, E., Wilson, T.W., 2017. Spatiotemporal oscillatory dynamics of visual selective attention during a flanker task. Neuroimage 156, 277–285.
Nagel, B.J., Herting, M.M., Maxwell, E.C., Bruno, R., Fair, D., 2013. Hemispheric lateralization of verbal and spatial working memory during adolescence. Brain Cognit. 82, 58–68.
Ng, H.B., Kao, K.L., Chan, Y.C., Chew, E., Chuang, K.H., Chen, S.H., 2016. Modality specificity in the cerebro-cerebellar neurocircuitry during working memory. Behav. Brain Res. 305, 164–173.
O'Hare, E.D., Lu, L.H., Houston, S.M., Bookheimer, S.Y., Sowell, E.R., 2008. Neurodevelopmental changes in verbal working memory load-dependency: an fMRI investigation. Neuroimage 42, 1678–1685.
Olesen, P.J., Macoveanu, J., Tegnér, J., Klingberg, T., 2007. Brain activity related to working memory and distraction in children and adults. Cerebr. Cortex 17, 1047–1054.
Papp, N., Ktonas, P., 1977. Critical evaluation of complex demodulation techniques for the quantification of bioelectrical activity. Biomed. Sci. Instrum. 13, 135–145.
Payne, L., Guillory, S., Sekuler, R., 2013. Attention-modulated alpha-band oscillations protect against intrusion of irrelevant information. J. Cognit. Neurosci. 25, 1463–1476.
Peters, B.D., Ikuta, T., DeRosse, P., John, M., Burdick, K.E., Gruner, P., Prendergast, D.M., Szeszko, P.R., Malhotra, A.K., 2014. Age-related differences in white matter tract microstructure are associated with cognitive performance from childhood to adulthood. Biol. Psychiatr. 75, 248–256.
Proskovec, A.L., Heinrichs-Graham, E., Wilson, T.W., 2016. Aging modulates the oscillatory dynamics underlying successful working memory encoding and maintenance. Hum. Brain Mapp. 37, 2348–2361.
Reuter-Lorenz, P.A., Jonides, J., Smith, E.E., Hartley, A., Miller, A., Marshuetz, C., Koeppe, R.A., 2000. Age differences in the frontal lateralization of verbal and spatial working memory revealed by PET. J. Cognit. Neurosci. 12, 174–187.
Rottschy, C., Langner, R., Dogan, I., Reetz, K., Laird, A.R., Schulz, J.B., Fox, P.T., Eickhoff, S.B., 2012. Modelling neural correlates of working memory: a coordinate-based meta- analysis. Neuroimage 60, 830–846.
Roux, F., Uhlhaas, P.J., 2014. Working memory and neural oscillations: alpha-gamma versus theta-gamma codes for distinct WM information? Trends Cognit. Sci. 18, 16–25.
Scherf, K.S., Sweeney, J.A., Luna, B., 2006. Brain basis of developmental change in visuospatial working memory. J. Cognit. Neurosci. 18, 1045–1058.
Taulu, S., Simola, J., 2006. Spatiotemporal signal space separation method for rejecting nearby interference in MEG measurements. Phys. Med. Biol. 51, 1759–1768.
Taulu, S., Simola, J., Kajola, M., 2005. Applications of the signal space separation method. IEEE Trans. Signal Process. 53, 3359–3372.
Thomason, M.E., Race, E., Burrows, B., Whitfield-Gabrieli, S., Glover, G.H., Gabrieli, J.D., 2009. Development of spatial and verbal working memory capacity in the human brain. J. Cognit. Neurosci. 21, 316–332.
Uusitalo, M.A., Ilmoniemi, R.J., 1997. Signal-space projection method for separating MEG or EEG into components. Med. Biol. Eng. Comput. 35, 135–140.
Van Veen, B.D., van Drongelen, W., Yuchtman, M., Suzuki, A., 1997. Localization of brain electrical activity via linearly constrained minimum variance spatial filtering. IEEE Trans. Biomed. Eng. 44, 867–880.
Vogan, V.M., Morgan, B.R., Powell, T.L., Smith, M.L., Taylor, M.J., 2016. The neurodevelopmental differences of increasing verbal working memory demand in children and adults. Dev. Cogn. Neurosci. 17, 19–27.
Wiesman, A.I., Heinrichs-Graham, E., McDermott, T.J., Santamaria, P.M., Gendelman, H.E., Wilson, T.W., 2016. Quiet connections: reduced fronto-temporal connectivity in nondemented Parkinson's Disease during working memory encoding. Hum. Brain Mapp. 37, 3224–3235.
Wilson, T.W., Heinrichs-Graham, E., Proskovec, A.L., McDermott, T.J., 2016. Neuroimaging with magnetoencephalography: A dynamic view of brain pathophysiology. Transl Res. 175, 17–36.
Wilson, T.W., Proskovec, A.L., Heinrichs-Graham, E., O'Neill, J., Robertson, K.R., Fox, H.S., Swindells, S., 2017. Aberrant neuronal dynamics during working memory operations in the aging HIV-infected brain. Sci. Rep. 7, 41568.
Zilles, D., Lewandowski, M., Vieker, H., Henseler, I., Diekhof, E., Melcher, T., Keil, M., Gruber, O., 2016. Gender differences in verbal and visuospatial working memory performance and networks. Neuropsychobiology 73, 52–63.